Appl. Phys. B 66, 47–52 (1998)

Applied Physics B
Lasers
and Optics

Cathode sputtered He-Zn laser

M. Jánossy, P. Mezei

Research Institute for Solid State Physics of the Hungarian Academy of Sciences, H-1525 Budapest POB 49, Hungary
(Fax: +36-1/395-9278)

Received: 23 July 1996/Revised version: 12 December 1996

Abstract. The operating characteristics of a slotted hollow cathode He-Zn laser were investigated. The Zn vapour was produced by sputtering in a slotted hollow cathode, consisting of four modules each of length 10 cm and slot size 2 mm × 5 mm. For excitation a pulsed discharge current of up to 10 A with a pulse duration 0.1–1 ms and pulse repetition rate of 5 p/s was used. The minimum threshold currents for the Zn II transitions observed were 0.4 A (758.8 nm), 1.6 A (747.9 nm), 0.7 A (492.4 nm) and 1.5 A (491.2 nm). These values are comparable with those of a similar sized heated laser. The influence of the discharge parameters and that of Ne, Ar and Kr on the laser intensity were studied in detail. A small quantity of Ar or Kr significantly increased the 492.4 nm, 491.2 nm and 758.8 nm laser power, while the power at 747.9 nm increased slightly. Addition of Ne quenched laser oscillation on the blue lines. The results are discussed on the basis of the excitation mechanisms for the different Zn II transitions. Quenching of the two blue laser lines is attributed to lower level excitation via charge transfer collisions with Ne ions. The cross section for this process is in the order of 10^{-15} cm^2, which indicates a possibility for laser action on the 210 nm Zn II line. The maximum laser power obtained was 78 mW for the infrared lines and 72 mW for the blue lines.

PACS: 42.55 H; 42.60 B; 52.20

Hollow cathode metal vapour lasers offer good possibilities for low power cw operation in the green, blue and ultraviolet region of the spectrum. This is due to the large variety of energy exchange collisions between noble gas ions (metastables) and metal atoms, available to excite the upper laser level [1]. The metal vapour can be produced by heating or by cathode sputtering. Heating has the advantage that the optimum lasing metal atom density can be reached. However, achieving a homogeneous stable metal vapour distribution raises several technical problems. Certain metals for uv operation (Cu, Ag, Au) [2] require heating to temperatures over 1000 °C, which raises technical difficulties. Although cathode sputtering is a simpler way to produce the metal vapour, the partial pressure obtained at technically feasible discharge currents is usually significantly below the optimum value. When using cathode sputtering the metal vapour density cannot be controlled independently of the discharge current. Room-temperature operation and the relative ease of obtaining a stable discharge has resulted in a wide application of this technique to hollow cathode lasers [2].

The hollow cathode He-Zn laser has been the subject of a large number of investigations [3–9]. These have been performed mostly using heating to produce the Zn vapour, since the optimum vapour pressure can be reached at tube temperatures around 400 °C. The only exception is the work of Karabut et al. [3], who reported operation of a He-Zn hollow cathode laser using cathode sputtering. Their paper contains little data which do not allow the properties of a cathode sputtered He-Zn laser to be determined.

The excitation mechanism of the Zn II 492.4 nm and 491.2 nm transitions has been considered to consist of two steps [10]:
Firstly charge transfer excitation by He ions to the $5d^2$D and $6p^2$P levels, which is followed by collisions of slow (thermal energy) electrons with the excited Zn ions, thus carrying the population to the $4f^2$F upper laser levels.

$$\mathrm{He}^+ + \mathrm{Zn} \rightarrow \mathrm{He} + \mathrm{Zn}^{+*} \quad (1)$$

$$\mathrm{e(slow)} + \mathrm{Zn}^{+*} \rightarrow \mathrm{e} + \mathrm{Zn}_\mathrm{L}^{+*} \quad (2)$$

where L indicates the upper laser level.

Iijima has investigated a hollow cathode He-Zn laser [11] and proposed that electron excitation from the Zn ion ground state is the dominant excitation process for the blue lines

$$\mathrm{e} + \mathrm{Zn}^+ \rightarrow \mathrm{e} + \mathrm{Zn}_\mathrm{L}^{+*} \quad (3)$$

Collins has suggested the possibility of producing population inversion at 210 nm ($4d^2\mathrm{D}_{5/2} - 4p^2\mathrm{P}_{3/2}$) in Ne-Zn, by charge transfer collisions with Ne ions to excite the upper $4d^2\mathrm{D}_{5/2}$ level [12]. He measured the cross section for this process to be 2.3×10^{-15} cm^2 [13]. No further investigations have been performed on this possibility, however. It is noted that the $4d^2\mathrm{D}_{5/2}$ level is also the lower level of the 492.4 nm laser transition.

In order to determine the capabilities of cathode sputtering and to investigate the questions connected with the excitation mechanisms mentioned we have carried out experiments on a He-Zn hollow cathode sputtering laser. Our investigations are concerned with the 758.8 nm ($5p^2P_{3/2}$ – $5s^2S_{1/2}$) and 747.9 nm ($4s^{22}D_{5/2}$ – $4p^2P_{3/2}$) infrared and the blue 492.4 nm ($4f^2F_{7/2}$ – $4d^2D_{5/2}$) and 491.2 nm ($4f^2F_{5/2}$ – $4d^2D_{3/2}$) laser transitions. The 758.8 nm line is believed to be excited by charge transfer collisions with He ions followed by a cascade, whereas the 747.9 nm line is pumped by Penning ionisation via He metastable atoms. The 747.9 nm line and the above mentioned 210 nm line have a common lower level. Energy level diagrams showing the Zn II laser transitions can be found e.g. in [1, 8, 13, 14]. In our experiments the effect of a gas additive (Ne, Ar, Kr) has been investigated in detail. The results obtained from the experiments support the two-step excitation mechanism previously proposed for the blue lines, but not a significant excitation by electron–Zn ground state ion collisions as suggested by Iijima. Also the cross section of the charge transfer collisions exciting the upper level of the 210 nm line by Ne ions was estimated to be of the order of 10^{-15} cm^2, our result of 3.5×10^{-15} cm^2 is in acceptable agreement with the measured value of [13]. The large cross section of the Ne ion-Zn atom collisions shows that it may be possible to obtain laser oscillation at this line. Significant output power was observed at all Zn II laser lines investigated, which suggests possible development of a cathode sputtered He-Zn laser for special applications.

1 Experimental

The transverse discharge slotted hollow cathode tube used in the experiments is depicted in Fig. 1. The size of the slot in each of the four Zn cathodes was 2 mm × 5 mm, and the section below was widened and a 1 mm diameter anode rod was inserted. The four 10 cm long cathodes arranged in series formed an active length of 40 cm. The cathodes were separated by the 1 cm anode holders since division of the discharge in this manner increases discharge stability [15]. The whole cathode-anode structure was placed in a pyrex glass tube. The discharge was excited by square current pulses of 0.1–1 ms duration with a peak current up to 10 A at a repetition rate of 5 p/s. The maximum average input power to the tube was 40 W and this resulted in a tube temperature of about 30 °C. The Zn vapour is considered to be produced entirely by cathode sputtering.

The optical resonator consisted of two 1.15 m radius mirrors placed 90 cm apart. The transmission of the output mirrors during the measurements was 0.5% for the infrared and 0.8% for the blue lines, except where otherwise specified in the text. A Spectra Physics model 404 power meter was used to measure the laser power. A Zeiss SPM2 monochromator served to select the different lines. An EMI 9558B photomultiplier was generally used, but the spontaneous emission on the Zn II 210 nm line was monitored using an EMI 6256S photomultiplier.

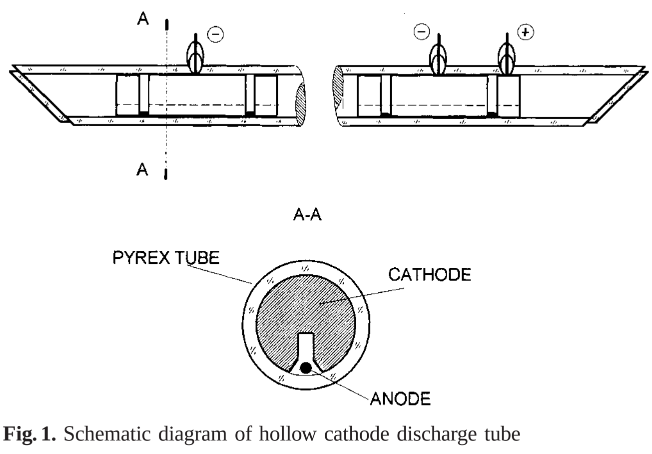

Fig. 1. Schematic diagram of hollow cathode discharge tube

2 Results

A pulse duration of 150 µs was generally used for the measurements. A typical laser pulse recorded at the blue lines, the current pulse and the corresponding voltage pulse for an active length of 40 cm are shown in Fig. 2. The figure shows that the onset of lasing is delayed by 30 µs, the laser power reaches its maximum at the end of the pulse, and the laser operation occurs for 40 µs in the afterglow. Exciting the discharge by longer pulses with durations up to 1 ms resulted in a constant laser power with approximately the value reached at 150 µs. This indicates that the 150 µs pulses produce conditions resembling cw operation.

The dependence of the laser intensity on the discharge parameters at the 758.8 nm, 747.9 nm infrared lines and at the 492.4 nm, 491.2 nm blue lines was investigated in detail. The threshold current for each of the lines was measured for discharge lengths of 10, 20, 30 and 40 cm. As Fig. 3 shows, the threshold currents for the 758.8 nm and 492.4 nm lines increase with discharge length. The lowest values, obtained for a 10 cm length, were 0.3 A and 0.7 A, respectively. The behaviour of the 491.2 nm line (not shown) was similar, the lowest threshold current being 1.6 A. However, the relationship at 747.9 nm was different, in that the threshold current decreased with increasing length, the lowest value being 1.6 A at a discharge length of 40 cm.

In all the following measurements an active length of 40 cm was used. The dependence of the laser power on He pressure for each of the laser transitions is shown in Fig. 4.

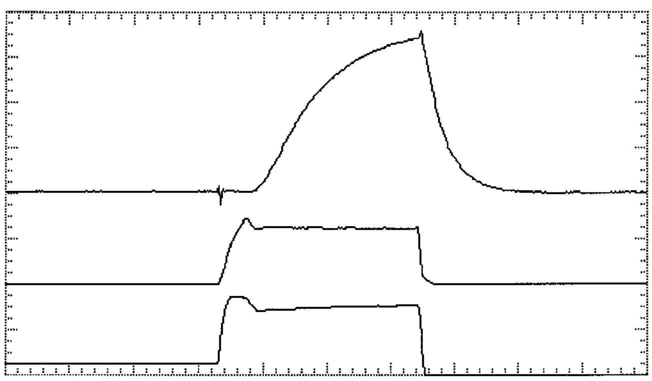

Fig. 2. Oscilloscope recording of 492.4 nm laser pulse (*top*), current pulse, 5 A (*middle*) and voltage pulse, 360 V (*bottom*). Exciting pulse length 150 µs. Scales: 3.4 mW/div, 4 A/div, 240 V/div, 50 µs/div. Gas pressure 15 mbar He + 0.4 mbar Ar

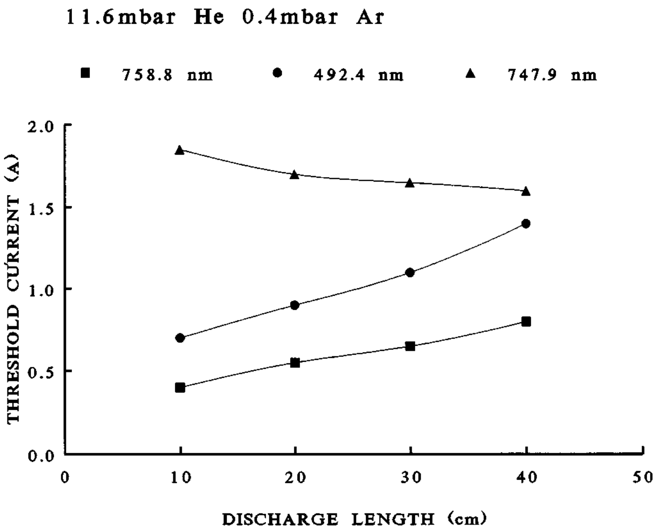

Fig. 3. Dependence of threshold currents of the different laser lines on discharge length. Output coupling: 0.5% (*infrared lines*), 0.8% (*blue lines*)

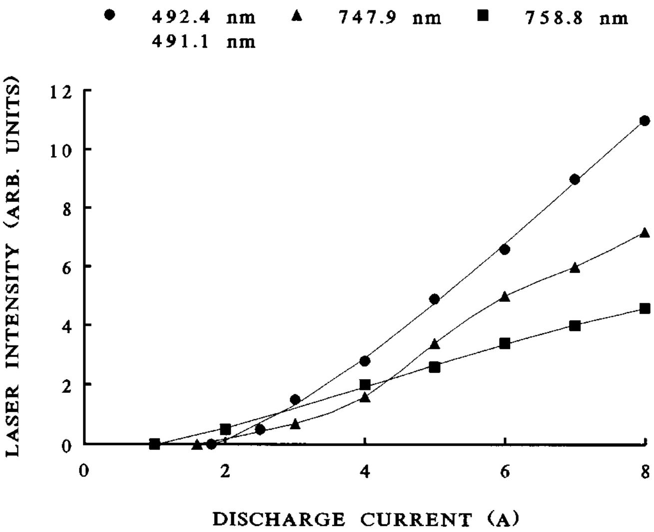

Fig. 5. Dependence of laser intensity on discharge current Gas fill data: 12 mbar He + 0.22 mbar Kr (*blue lines*), 9 mbar He + 0.4 mbar Ar (*infrared lines*)

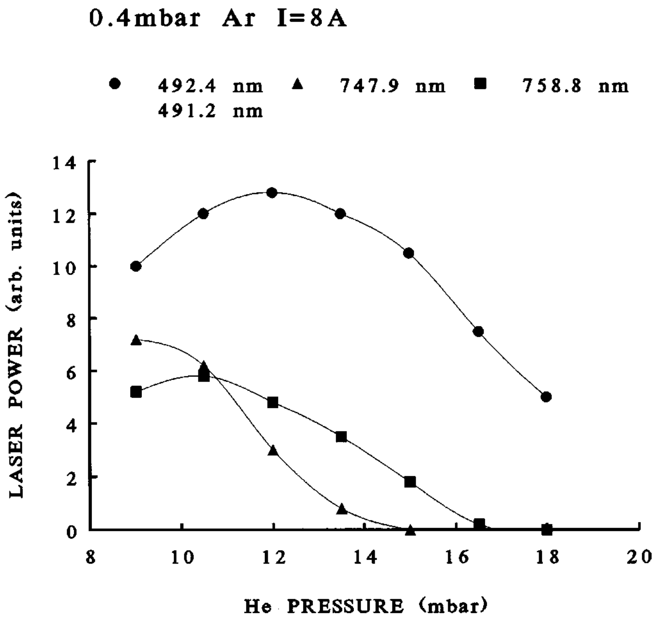

Fig. 4. Dependence of laser power on He pressure

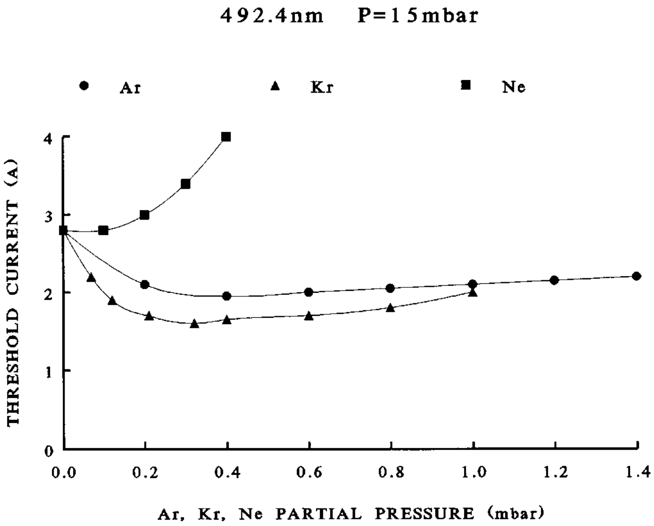

Fig. 6. Dependence of 492.4 nm threshold current on Ne, Ar and Kr partial pressure

The measurements were carried out for a discharge current of 8 A and Ar at a partial pressure of 0.4 mbar was added to the He to increase cathode sputtering. Figure 4 shows that the optimum He pressure is 12 mbar for 492.4 nm, 10.5 mbar for 758.8 nm and is lower than 9 mbar for 747.9 nm.

The relationship between the laser power and the discharge current is plotted in Fig. 5. Figure 5 indicates that laser power for each line increases with the discharge current and that no saturation was observed at a He pressure near optimum.

The effect of admixing Ar, Kr and Ne on the threshold current and the laser power was investigated in detail. The relationship between the threshold current for the 492.4 nm transition and the partial pressure of Ar, Kr and Ne is plotted in Fig. 6. In these measurements the total pressure was kept constant at 15 mbar. Figure 6 shows that the threshold current decreases to 2 A for 0.4 mbar Ar and to 1.6 A for 0.3 mbar Kr. However, when Ne was added to the discharge the threshold current increased rapidly and for Ne at 0.4 mbar the laser operation ceased.

The variation of the laser power for the blue lines (492.4 nm and 491.2 nm) with changing the partial pressure of Ar, Kr and Ne is shown in Fig. 7. The total gas pressure was 15 mbar and the current was 8 A. The laser power increases significantly when Ar or Kr is added to the discharge but drops rapidly to zero however, when Ne is added as mentioned earlier. The maximum increase of laser power is by a factor of 3 and occurs at 0.4 mbar Ar or 0.3 mbar Kr. The laser power shows a broad maximum and after this decreases slowly with increasing partial pressure of Ar or Kr.

The laser output power at 758.8 nm as a function of the partial pressure of Ar, Kr and Ne for a total pressure of 12 mbar and a current of 8 A is plotted in Fig. 8. The laser intensity increases when any one of the three gases is added to He. The strongest increase, by a factor of 3.5, was found at

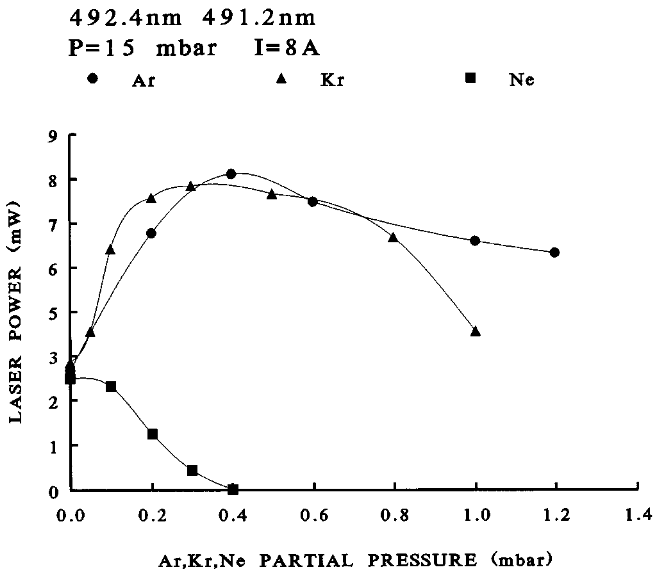

Fig. 7. Dependence of laser power at the blue lines on Ar, Kr and Ne partial pressure

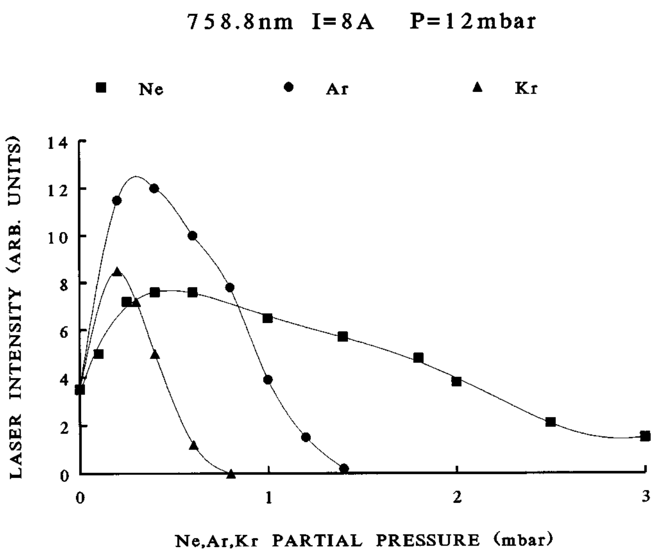

Fig. 8. Dependence of 758.8 nm laser intensity on Ne, Ar and Kr partial pressure

0.4 mbar Ar partial pressure. When Ne is added laser operation was observed over a broad range of Ne partial pressures, and oscillation occurred up to 3 mbar Ne.

The relationship between the 747.9 nm laser power and changes in the partial pressure of Ar, Kr and Ne, for the same conditions as in Fig. 8, is shown in Fig. 9. As can be seen from the figure the addition of Ar increases laser power by about 20% and Kr by 50%, respectively. The progressive addition of Ne results in a continuous decrease of laser power, and oscillation ceased at 1.4 mbar Ne partial pressure.

The maximum output power of the laser was measured for the optimum gas fill for each of the different transitions and at 10 A discharge current. A 1.5% transmission mirror was used for the blue lines and a 1% mirror for the infrared ones, respectively. The maximum values obtained for the laser power were 30 mW (758.8 nm), 48 mW (747.9 nm), 54 mW (492.4 nm), 18 mW (491.2 nm).

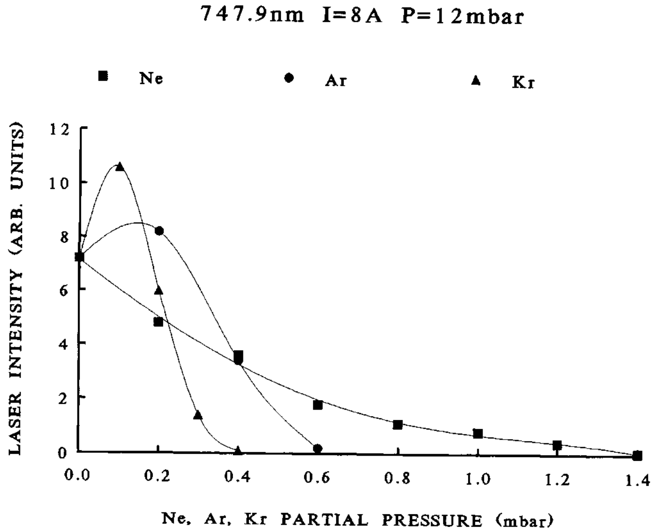

Fig. 9. Dependence of 747.9 nm laser intensity on Ne, Ar and Kr partial pressure

In order to obtain data on the quenching of laser oscillation on the blue lines caused by the addition of Ne, the spontaneous intensity of each of the 491.2 nm and 210 nm Zn II lines was measured as a function of Ne partial pressure. These two lines allow the excitation processes to be characterised through the dependence of spontaneous emission on the Ne partial pressure. The spontaneous 492.4 nm line could not be resolved by the monochromator due to the strong neighbouring He line at 492.1 nm. In these measurements the total pressure was 15 mbar, and the discharge current 6 A. The results of measurements can be seen in Fig. 10. At low Ne pressures the intensity at 210 nm increases more steeply than that at 491.2 nm, indicating a strong increase of lower level population of the blue lines. The 491.2 nm line shows a maximum at 1 mbar Ne. A further increase in the Ne partial pressure causes the 491.2 nm intensity to decrease slowly. On the other hand the initially strong increase of 210 nm intensi-

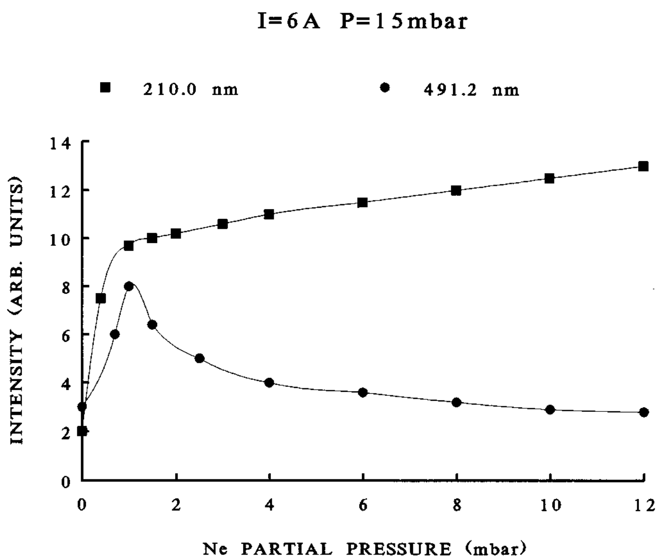

Fig. 10. Dependence of Zn II 210 nm and 491.2 nm spontaneous intensity on Ne partial pressure

ty slows down above 2 mbar Ne but continues to increase with Ne pressure up to 12 mbar, the highest partial pressure of Ne used in these experiments.

3 Discussion

The operating characteristics of the hollow cathode sputtered He-Zn laser transitions are connected with the discharge processes and the excitation mechanisms.

The onset of laser oscillation is delayed with respect to the beginning of the current pulse as can be seen in Fig. 2. The delay was observed to vary with the different laser transitions. Typical delay values in a gas mixture of 15 mbar He and 0.4 mbar Ar at 4 A discharge current were 30 μs (758.8 nm), 120 μs (747.9 nm) and 40 μs (492.4 nm). The pumping rates for the laser transitions are proportional to the concentration of ground state Zn atoms. Thus, the main reason for the delay is the time necessary for the sputtered Zn vapour to diffuse from the cathode wall to the discharge region where laser operation occurs. However, the differences in the time delays for the laser transitions are a consequence of the different excitation mechanisms, which result in different gains for each of the laser lines. The output power for the 747.9 nm line is very low at the 15 mbar gas pressure used for the measurements, which indicates a very low gain, thus in this case a long time is needed to reach a density of Zn atoms sufficient for laser threshold.

The threshold currents for the different laser transitions falling in the range of 0.5–1.5 A are not much higher than the values of 0.2–0.6 A obtained in a heated He-Zn laser that has a similar size hollow cathode bore [8]. The active length in [8] was 50 cm, and output mirror couplings were 1% (747.9 nm), 3% (758.8 nm) and 2% (492.4 nm), respectively. The optimum He pressures fall in the range of 10–12 mbar (Fig. 4) and are lower than the values of 15–40 mbar for the heated He-Zn laser of reference [8]. This is due to the fact that the laser power is very sensitive to the Zn vapour pressure. At lower He pressures the efficiency of cathode sputtering in producing Zn vapour significantly increases. The presence of a higher density of Zn atoms increases laser power more than the decrease due to the He pressure being lower than the optimum corresponding to the heated laser of [8].

The relatively low threshold currents occurring in the cathode sputtered laser are connected to the operation at low He pressures. At these He pressures the discharge is used very efficiently since it is practically confined within the hollow cathode slot. Thus, all the current is used only for sputtering and laser excitation, since no current flows inside the 0.5 mm narrow gaps between the electrode parts or to any other cathode surface part. These facts were readily confirmed by visual inspection of the discharge tube.

In the heated He-Zn laser of [8] saturation of the laser power for the two infrared lines with increasing current was observed. This is not the case in the cathode sputtered laser where saturation did not occur. The lack of saturation is explained by the Zn vapour density being lower than the optimum. Due to this the He ion and metastable densities exciting these transitions are not saturated and increase continuously with increasing discharge current. At the blue lines the laser power dependence on discharge current was similar in the heated and in the cathode sputtered lasers, in both cases laser power increased up to the highest current values used. These similar dependences are most likely connected with the fact that low-energy electrons are involved in the excitation of the blue transitions. The density of the low-energy electrons increases continuously with increasing discharge current, irrespectively of the way in which the Zn vapour is produced.

The increase of laser power by the addition of Ar, Kr or Ne in general is due to the increase of Zn density by enhanced cathode sputtering. This results from the ions of the admixed gas gaining higher energies due to their longer mean free path [16].

The broad maximum of the dependence of laser power of the blue lines on the partial pressure of Ar or Kr, and the slow decrease in the laser power at higher partial pressures, can be explained in a straightforward manner on the basis of the accepted excitation mechanism involving He ions in the first and slow electrons in the second step. The upper-level population of the blue lines is proportional to the product of slow electron density and He ion density. The addition of Ar or Kr to He increases the density of slow electrons because of the electron impact ionisation rate of Ar and Kr is higher than that of He. This increase in the slow electron density more or less offsets the decrease in the He ion density due to the reduction of the number of high-energy electrons [16]. These two changes together result in only a relatively small decrease of laser power at the higher Ar and Kr partial pressures. Concurrently, the addition of Ar or Kr causes the 758.8 nm laser power to exhibit a more rapid decrease since only He ions are involved in the excitation of this transition.

The 747.9 nm transition shows no increase in the laser power when Ne is added to the He (Fig. 9). This line is excited by Penning collisions with He metastable atoms. The absence of a maximum in the laser power-Ne partial pressure dependence is attributed to the decrease of He metastable density resulting from collisions of the second kind with Ne atoms. This process is dominant over the increase of Zn vapour pressure due to the enhanced cathode sputtering caused by Ne ions.

It can be concluded from our experimental results that a significant population of the upper $4f\,^2F_{7/2,5/2}$ levels of the blue laser transitions occurring by the electron-Zn ion collision mechanism suggested by Iijima [11] is unlikely. This conclusion is supported by the following two observations:

1. Laser oscillation occurs in the afterglow over times of 40 μs, which is typical for excitation by long-lived atomic species.
2. The dependence of the laser power on the Ar and Kr partial pressures can be clearly explained on the basis of the presently accepted excitation mechanism involving He ions and slow electrons. At high partial pressures of Ar or Kr the density of high energy electrons which is necessary in case of electron-Zn ion collisions decreases and this would be expected to result in a strong decrease of laser power. However, this was not observed as the laser power exhibited only a slow decline.

As mentioned in the introduction Collins [12, 13] has suggested the possibility of charge transfer excitation of the $4d^2D_{5/2}$ level by Ne ions on the basis of a close energy coincidence, the energy difference between the Ne ion (21.56 eV) and the $4d^2D_{5/2}$ level (21.41 eV) is 0.15 eV. Thus the quenching of laser oscillation observed at the two blue 492.4 nm and 491.2 nm lines is attributed to lower level excitation by this process. The great increase in the spontaneous 210 nm intensity at low Ne partial pressures supports this statement. The fact that a small amount (0.4 mbar) of Ne completely stops the blue laser oscillation indicates a large cross-section for the Ne ion-Zn atom charge transfer collisions. Based on a rate equation model this cross-section has been estimated [17]. In the model it was assumed that populations of the upper and lower laser levels are equal at the Ne partial pressure where oscillation stops and also that He and Ne ion densities are proportional to their partial pressures. The gas temperature in the discharge was estimated to be ~ 550 K, this value was obtained by extrapolation of data measured in [18]. As a result of the calculation the cross-section value was found to be $\sigma = 3.5 \times 10^{-15}\,\mathrm{cm}^2$. This value is in acceptable agreement with the value $2.3 \times 10^{-15}\,\mathrm{cm}^2$ measured by Collins [13]. The difference can be attributed to the approximations used in our model. The lower level of the 210 nm line is also the lower level of the Penning ionisation excited 747.9 nm line, which transition is depopulated by the strong 202.5 nm transition. The large cross section for upper-level excitation of the 210 nm line and the existing lower-level depopulation suggests the possibility for population inversion and laser oscillation at 210 nm.

4 Conclusions

The operating parameters of a cathode sputtered hollow cathode He-Zn laser have been investigated. Threshold currents not very much higher than those obtained in a similar size heated He-Zn laser have been measured. This result is explained by the match of optimum laser gas pressure with that pressure needed for efficient operation of the hollow cathode discharge in the 2 mm $\times$ 5 mm size slot. The effect of admixing Ar, Kr and Ne on each of the laser transitions was studied in detail. It was found that, in the case of transitions involving charge transfer in their excitation mechanism, the addition of Ar or Kr significantly increases the laser power due to enhanced cathode sputtering. The quenching of the laser operation on the blue 492.4 nm and 491.2 nm lines by the addition of Ne is attributed to lower-level excitation via charge transfer collisions with Ne ions. The cross section for this process was estimated to be in the order of $10^{-15}\,\mathrm{cm}^2$ which is in acceptable agreement with that obtained by Collins. Consideration of this large cross section together with existing lower-level depopulation indicates a possibility for laser action on the 210 nm Zn II transition. Recent work on high-voltage variants of the hollow cathode have shown their superiority to the conventional hollow cathode for charge transfer pumped lasers [19]. Application of high-voltage hollow cathodes results in higher gains, and may thus facilitate the task of achieving laser operation on the 210 nm line.

The laser operated in a stable and reproducible manner in the course of the investigations. Stable operation was achieved even when using a pulse duration of 0.5 ms at an output power as high as 70 mW. The experiments have shown that cathode sputtering is a convenient way to operate a He-Zn laser, thus making it possible to develop cathode sputtered He-Zn lasers for special applications.

Acknowledgements. Thanks are due to Mr. J. Tóth, Mr. E. Sárközi, Mrs. T.J. Forgács and Mr. Gy. Császár for construction of the discharge tube and to Mr. J. Takács for supplying the Zn metal. This work was supported by the Hungarian Science Foundation OTKA, grant T-4227.

References

1. W.B. Bridges: *Methods of Experimental Physics, Quantum Electronics A, Atomic and Ionic Gas Lasers* (Academic Press, New York 1979) p. 31
2. D.C. Gerstenberger, R. Solanki, G.J. Collins: IEEE J. Quantum Electron. **16**, 820 (1980)
3. E.K. Karabut, V.S. Mihalevskij, V.F. Papakin, M.F. Sem: Z. Tech. Fiz. **39**, 1923 (1969)
4. Y. Sugawara, Y. Tokiwa: Jpn. J. Appl. Phys. **9**, 588 (1970)
5. Y. Sugawara, Y. Tokiwa, T. Iijima: Jpn. J. Appl. Phys. **9**, 1537 (1970)
6. R.C. Jensen, G.J. Collins, W.R. Bennett Jr.: Appl. Phys. Lett. **18**, 50 (1971)
7. T. Iijima, Y. Sugawara: J. Appl. Phys. **45**, 5091 (1974)
8. J.A. Piper, P. Gill: J. Phys. D **8**, 127 (1975)
9. T. Iijima, Y. Sugawara: Jpn. J. Appl. Phys. **16**, 365 (1977)
10. J.M. Green, G.J. Collins, C.E. Webb: J. Phys. B **6**, 1445 (1973)
11. T. Iijima: Jpn. J. Appl. Phys. **15**, 1395 (1976)
12. G.J. Collins: Thesis, Yale University, New Haven USA (1970) p. 110
13. G.J. Collins: J. Appl. Phys. **42**, 3812 (1971)
14. G.J. Collins: J. Appl. Phys. **44**, 4633 (1973)
15. K. Rózsa: Z. Naturforsch. **35a**, 649 (1980)
16. Z. Donkó, M. Jánossy: J. Phys. D **25**, 1323 (1992)
17. M. Jánossy, P. Mezei (to be published)
18. L. Csillag, M. Jánossy, K. Rózsa: Appl. Phys. B **52**, 90 (1991)
19. R.C. Tobin, K.A. Peard, G.H. Bode, K. Rózsa, Z. Donkó, L. Szalai: IEEE J. Select. Topics Quantum Electron. **1**, 805 (1995)